Low ozone concentrations promote *in vitro* preservation of explanted articular cartilage: an ultrastructural study

Giada Remoli,[1] Chiara Rita Inguscio,[1] Federico Boschi,[2] Gabriele Tabaracci,[3] Manuela Malatesta,[1]* Barbara Cisterna[1]*

[1]Department of Neurosciences, Biomedicine and Movement Sciences, University of Verona
[2]San Rocco Clinic, Montichiari (BS)
[3]Department of Engineering for Innovation Medicine, University of Verona, Italy

**These authors contributed equally*

ABSTRACT

Ozone (O_3) is an oxidizing natural gas widely applied as adjunctive therapeutic treatment for a variety of pathological conditions. Currently, O_3-based therapies rely on the low-dose concept *i.e.*, the administration of low O_3 concentrations able to induce a mild oxidative stress stimulating antioxidant and anti-inflammatory response without causing cell damage. In addition, low O_3 concentrations are thought to activate cellular and molecular mechanisms responsible for analgesic and regenerative effects. Due to these properties, in the last decade interest has arisen in the fields of orthopedics and regenerative medicine on the potential of O_3 to counteract joint diseases involving cartilage degeneration. In this pilot study, we have explored the anti-degenerative potential of O_3 on knee articular cartilage explanted from a healthy adult rabbit and maintained *in vitro*. Light and transmission electron microscopy were used to monitor chondrocyte and extracellular matrix features of cartilage samples undergoing O_3 treatment every three days for two weeks. Results demonstrated that low O_3 concentrations act on chondrocytes and the molecular components of the extracellular matrix of articular cartilage explants, significantly improving their preservation under *in vitro* conditions, likely by promoting both protective and pro-regenerative pathways. This opens promising perspectives for further investigations on the therapeutic potential of O_3 for the treatment of cartilage degeneration not only as painkilling and anti-inflammatory agent but also as a cartilage regenerative agent.

Key words: chondrocyte; pericellular matrix; interterritorial matrix, collagen fibrils; low-dose ozone; transmission electron microscopy.

Correspondence: Manuela Malatesta, Department of Neurosciences, Biomedicine and Movement Sciences, University of Verona, Strada Le Grazie 8, 37134 Verona, Italy. E-mail: manuela.malatesta@univr.it

Contributions: Giada Remoli, data acquisition and analysis, manuscript drafting; Chiara Rita Inguscio, data acquisition and analysis; Federico Boschi, data analysis, statistics and interpretation; Gabriele Tabaracci, conception of the work, manuscript reviewing; Manuela Malatesta, design of the work, data analysis, manuscript drafting and reviewing; Barbara Cisterna, design of the work, data analysis, manuscript drafting and reviewing. All authors read and approved the final version of the manuscript and agreed to be accountable for all aspects of the work.

Conflict of interest: the authors declare no competing interests and all authors confirm accuracy.

Availability of data and materials: the datasets used and/or analyzed during the current study are available upon reasonable request from the corresponding author.

Introduction

Ozone (O_3) is a gas naturally occurring in the Earth atmosphere. It is made of three oxygen atoms and is highly instable, rapidly decomposing into oxygen (O_2). The strong oxidizing power of O_3, which makes it potentially harmful for animal and human health, was discovered in the nineteenth century[1,2] and was soon exploited for medical purposes. In particular, O_3 is being commonly used as a disinfectant agent.[3,4] Thanks to the technological advancement for the production and management of medical O_3, in the last century, O_3 has become a widely applied adjunctive therapeutic treatment -as a gaseous O_2- O_3 mixture or as ozonated oil or water- for a variety of pathological conditions in different human and veterinary medical fields (*e.g.*, angiology, dentistry, dermatology, neurology, orthopedics).[5-18] Currently, O_3-based therapies rely on the low-dose concept *i.e.*, the administration of low O_3 concentrations:[19] in fact, scientific research has demonstrated that low O_3 concentrations (from 10 to 50 µg O_3/mL O_2) exert therapeutic effects by inducing a mild oxidative stress [20] (called eustress [21,22]) which does not cause cell damage but is able to activate protective molecular pathways through the activation of the transcription nuclear factor erythroid 2-related factor 2 (Nrf2), the master regulator of cellular redox homeostasis.[23-27] Experimental findings have demonstrated that low O_3 concentrations not only stimulate antioxidant and anti-inflammatory response but also activate cellular and molecular mechanisms responsible for analgesic and regenerative effects (recent review in [28]).

Due to these properties, in the last decade interest has arisen in the fields of orthopedics and regenerative medicine on the potential of O_3 to counteract joint diseases involving cartilage degeneration.

Articular cartilage is a highly specialized connective tissue providing a smooth, lubricated surface to bony ends for articulation of diarthrodial joints. It is composed of an only resident cell type called chondrocytes, which are surrounded by a dense extracellular matrix distinct into pericellular matrix (thin layer adjacent to the chondrocyte membrane), territorial matrix (a basketlike network around the chondrocytes, which is hardly distinguishable from pericellular matrix in adult individuals), and interterritorial matrix (the major portion of matrix away from the chondrocytes).[29] The pericellular matrix is made of a network of granules and fine fibrils corresponding to proteoglycans (mostly aggrecan) and hyaluronan, respectively, which, together with collagen (mostly type VI) and glycoproteins, are connected to the chondrocyte surface regulating matrix assembly and turnover.[29-32] The intercellular matrix contains a fibrous network made of different collagen molecules (although more than 90% of the total is type II collagen) and proteoglycans, while other noncollagenous proteins and glycoproteins are present in low amounts; these molecular components are located in the interfibrillar space and allow high amounts of water to be retained, thus providing articular cartilage with the biomechanical properties necessary to resist compressive loads.[31] Chondrocytes are spatially ordered in the matrix, and are responsible for the synthesis and degradation of both the fibrillar and the amorphous components of the extracellular matrix, thus ensuring its turnover and repair.[33] However, the intrinsic features of the tissue (*i.e.*, absence of blood vessels, lymphatics, and nerves; scarce proliferation potential of chondrocytes) limit the self-healing capacity when damage occurs. For the same reasons, damaged articular cartilage is very difficult to cure, thus representing a great medical challenge.

A number of clinical observational studies have reported beneficial effects of the intra-articular administration of O_3 in limiting symptoms of debilitating conditions such as osteoarthritis, gouty arthritis or facet joint syndrome, characterized by chronic pain and diminished quality of life (reviews in [9,34-38]). However, the O_3 healing effectiveness is still a matter of debate due to the relatively recent development of this therapeutic approach as well as to the great heterogeneity of the protocols used.[39-41]

Actually, the scarce experimental evidence of the effects of O_3 on the articular cartilage is the main obstacle for a wide clinical acceptability and exploitation of O_3 treatment in joint diseases.[42-48] This basic knowledge would be crucial to understand if the positive response to O_3 treatment reported in patients suffering from articular cartilage diseases only depends on the analgesic and anti-inflammatory properties of O_3 or is also due to cartilage tissue healing.

Based on the previously demonstrated effectiveness of low O_3 concentrations to improve the structural preservation of tissue explants,[49] in this pilot study we have explored the anti-degenerative potential of O_3 on knee articular cartilage explanted from a healthy adult rabbit and maintained *in vitro*. Light and transmission electron microscopy were used to monitor chondrocyte and extracellular matrix features of cartilage samples undergoing treatment with gaseous O_2-O_3 mixture every three days for two weeks.

Materials and Methods

Articular cartilage sampling and treatment

Knee articular cartilage was harvested from a skeletally mature rabbit (18 months of age) bought in a local butcher for food consumption. Cartilage samples of about 1 mm in thickness were removed with a scalpel from the underlying subchondral bone of femoral condyles and tibial plateau within 1 h of slaughter. The cartilage samples were immediately washed with 0.1 M phosphate buffered saline (PBS) pH 7.4 and then placed in 35 mm plastic dishes (8 samples per dish) containing 3 mL of DMEM medium supplemented with 1 g/L glucose, 10% fetal bovine serum and 2% penicillin/streptomycin. The explanted samples were put into an incubator at 37°C in a 5% CO_2 humidified atmosphere, and allowed to stabilize overnight in the medium before starting the experiment. Explants were maintained in culture medium for increasing times (for up to 12 days), replacing the medium every third day.

Some explants were treated with O_2-O_3 gas mixtures produced from medical-grade O_2 by an Ozonline E80 apparatus (Multisales Srl, Bergamo, Italy), which allows real-time control of O_3 concentration and gas flow rate. O_3 was used at the concentration of 16 µg O_3/mL O_2, which is currently administered in the clinical practice for intra-articular injections and experimentally proved its antioxidant effect [25]. Cartilage samples of each experimental condition were weighted and then suspended in medium (30 mg of cartilage tissue/mL) in a 20 mL O_3-resistant polypropylene syringe (Terumo Medical Corporation, Somerset, NJ, USA). A volume of gas equal to medium volume was then collected into the syringe through a sterile filter to avoid contamination. The sample was gently mixed with the gas mixture for 10 min according to Larini *et al*.[50] The samples were then placed in plastic dishes containing fresh medium and put into the incubator.

Gas treatments were applied at the beginning of the experiment (t0), and at days 3, 6, and 9 (referred to as t3, t6, and t9, respectively). Control samples underwent the same handling at the same timepoints without exposure to the O_2-O_3 gas mixture. Treated and control samples were processed for light and transmission electron

microscopy at t3, t6 and t12. Samples at t0 served as control of the cartilage native features. A graphical description of the experiment is reported in Figure 1.

Sample processing for microscopy analyses

Treated and control cartilage samples were fixed for 2 h at 4°C with 2.5% glutaraldehyde and 2% paraformaldehyde in 0.1 M phosphate buffer pH 7.4, washed and post-fixed at 4°C for 30 min with 1% OsO_4. The samples were then dehydrated with acetone and embedded in Epon resin (all reagents were purchased from Electron Microscopy Sciences, Hatfield, PA, USA). For light microscopy analysis, sections of 2 µm in thickness were cut with a Reichert Jung 2050 and placed onto glass slides. For transmission electron microscopy analysis, 70-90 nm-thick ultrathin sections were cut with a Reichert Jung Ultracut and collected on 200 mesh copper grids (Electron Microscopy Sciences).

Light microscopy analysis

Toluidine blue is known to stain proteoglycans in the cartilage extracellular matrix due its high affinity for their sulfate groups, and the degree of positive staining is commonly used to assess the amount of these molecules *in situ*.[51,52] Therefore, the sections collected on glass slides were stained with an aqueous solution of 0.1% toluidine blue for 2 min at room temperature. To ensure homogeneity in staining procedure, all samples were treated in the same run. Cartilage samples were observed with an Olympus BX51 microscope equipped with an Olympus Camedia C-5050 digital camera (Olympus Italia Srl, Segrate, MI, Italy). To evaluate staining intensity, images of a total of 15 randomly selected fields (20×) were taken in 4 sections of each experimental condition and analyzed with a MATLAB code (MathWorks, Inc., Natick, MA, USA) developed to measure the mean RGB values. Two thresholds were used to exclude the darkest and brightest pixels. An expert author carried out blind assessment of the measured area by excluding the pixels with intensity above and below the thresholds. Staining intensity index was calculated by subtracting the obtained RGB values from 255 (the higher the value, the higher the extracellular matrix density).

Transmission electron microscopy analysis

Ultrastructural morphological analysis of chondrocytes and extracellular matrix components of cartilage samples was performed on ultrathin sections stained with Reynolds' lead citrate (Electron Microscopy Sciences) for 2 min. Samples were observed with Philips Morgagni transmission electron microscope (FEI Company Italia Srl, Milan, Italy) operating at 80 kV, and image acquisition was made with a Megaview III camera (FEI Company Italia Srl). In addition, a morphometric analysis of some cellular and extracellular components was carried out using ImageJ software (NIH). To ensure sampling homogeneity, measurements were performed in the intermediate zone of the articular cartilage (which constitutes about 50% of the overall thickness), avoiding the surface layer and the deeper region facing the subchondral bone.[29] The areas of cytoplasmic regions and of residual bodies occurring therein were measured in 10 cells per sample (x 8,900), then the percentage of residual body (total residual body area/cytoplasmic area x 100) was calculated. The length of chondrocyte surface was measured both including (real length of the chondrocyte profile) and excluding (corresponding linear length) cell protrusions in 30 cells per sample (X 18,000); the ratio between the two values was then calculated in order to obtain an index of cell surface irregularity (the higher the value, the rougher the cell). In the same images, the density of granules in the pericellular matrix network (number of granules/µm^2) was assessed as an index of the protein lattice spacing. In the interterritorial matrix, 100 longitudinally sectioned collagen fibrils were evaluated for their size and D band length (periodicity) (x44,000). For each fibril, one measure of size and two measures of band length were taken.

Statistical analysis

Data for each variable were pooled according to the experimental condition and presented as mean ± standard error of the mean (SE). Statistical significance was assessed by the Kruskal Wallis test followed, in case of significance, by the Mann Whitney test for pairwise comparison with Bonferroni correction. Significance was set at $p \leq 0.05$.

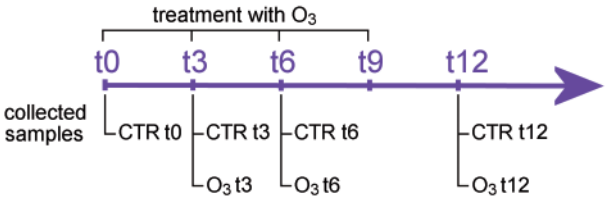

Figure 1. Graphical description of the experiment.

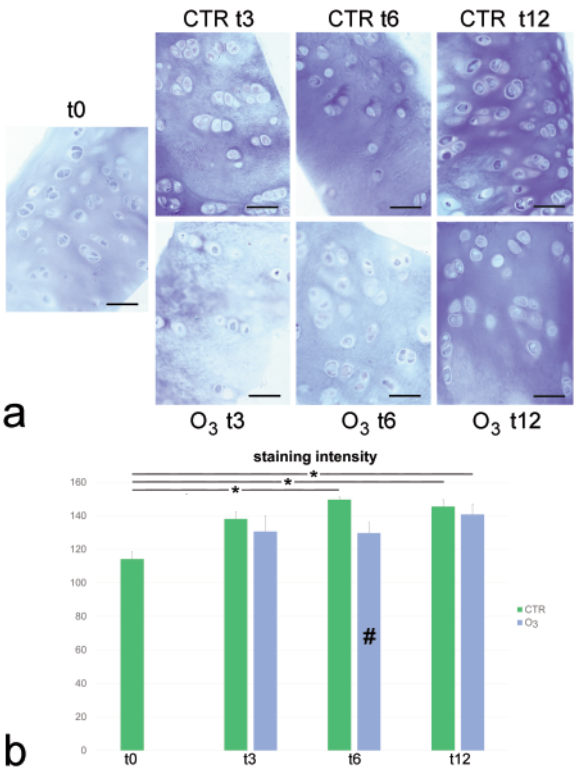

Figure 2. a) Bright field microscopy images of articular cartilage; toluidine blue staining; scale bars: 100 µm. **b**) Results of staining intensity evaluation; mean values ±SE; asterisk indicates statistically significant difference from t0; hashtag indicates statistically significant difference from control (CTR) of the same timepoint.

Results

Light microscopy analysis

At light microscopy, all samples showed the typical morphological features of articular cartilage, with a thin superficial zone containing small flattened chondrocytes oriented parallel to the articular surface, an intermediate zone containing roundish chondrocytes scattered in the matrix, and a deep zone containing columns of chondrocytes oriented perpendicularly to the articular surface. The extracellular matrix had an amorphous appearance, without evident fibrillar structures (Figure 2). No difference in the histological organization was observed among the experimental groups. Quantitative evaluation of toluidine blue staining revealed that in control samples the staining intensity was significantly higher at t6 and t12 than at t0; O_3-treated samples at t3 and t6 showed values similar to t0, but at t12 the staining intensity significantly increased.

Transmission electron microscopy analysis

At t0, the ultrastructural morphological analysis demonstrated well preserved chondrocytes characterized by a roundish nucleus with a few heterochromatin clumps. Abundant rough endoplasmic reticulum (RER), well-developed Golgi apparatuses and ovoid mitochondria along with small deposits of glycogen granules occurred in the cytoplasm (Figure 3 a,b). The pericellular matrix surrounding the chondrocytes was made of a network of granules and fine fibrils corresponding to proteoglycans (mostly aggrecan) and hyaluronan, respectively (Figure 3c). The interterritorial matrix contained many single collagen fibrils showing the typical banding and oriented in different directions within an amorphous environment (Figure 3d).

In control samples, a cytoplasmic accumulation of glycogen deposits was observed at t3 and t6, and some residual bodies and multilamellar bodies appeared at t3, becoming much more abundant at t6 (Figures 4 a,b and 5 a,b). At t12, many chondrocytes contained numerous residual bodies and lipid droplets, while other chondrocytes were necrotic (Figure 6 a,b). In the pericellular matrix, the fibro-granular network appeared as loosened with scarce granules in all control samples (Figures 4c, 5c, 6c). The interterritorial matrix did not show evident morphological differences with t0 at all timepoints, but an increase of collagen fibril thickness was found at t3 and t6 (Figures 4d, 5d, 6d).

In O_3-treated samples, chondrocytes were morphologically similar to t0 at all timepoints, with well-preserved cell organelles (Figures 7 a,b; 8 a,b; 9 a-c). The only exception was RER at t12, which sometimes appeared as collapsed and showed scarce ribosomes (Figure 9 a-c). In addition, some glycogen accumulation, and a few residual and multilamellar bodies were present (Figures 7 a,b; 8 a,b; 9 a-c). The pericellular matrix was similar to t0 at t3 and t6 (Figures 7c and 8c), but it became loosened at t12 (Figure 9d). The interterritorial matrix appeared similar to t0 at all timepoints (Figures 7d; 8d; 9e).

Morphometric analysis demonstrated that the percentage of residual bodies occurring in control samples at t3 was similar to t0, but significantly increased at t6 and t12; in O_3-treated samples the values at t3 and t6 were similar to t0, whereas at t12 the percentage

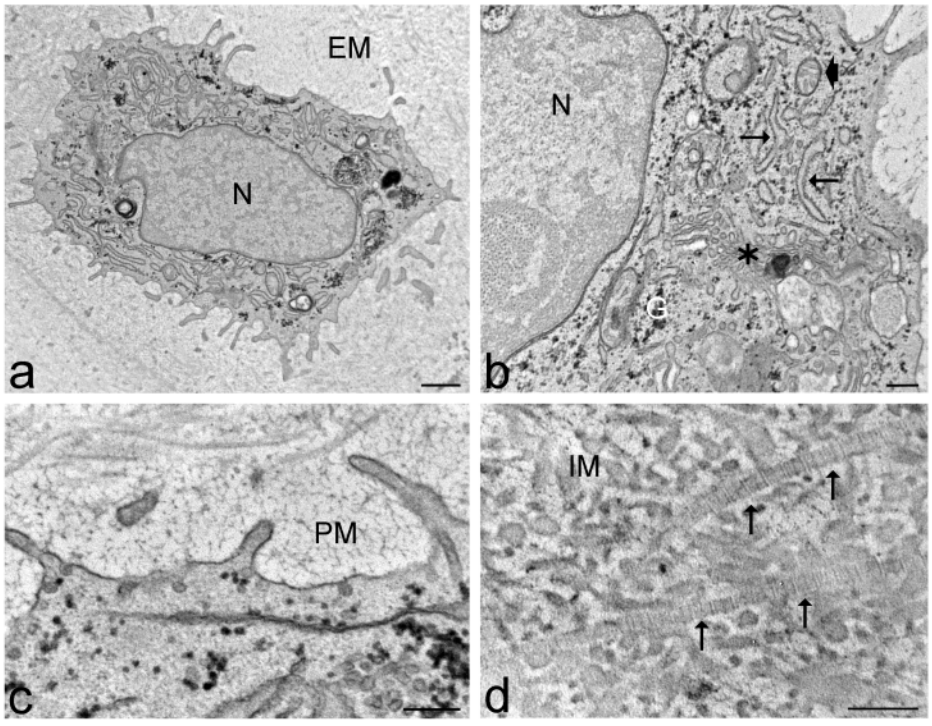

Figure 3. Transmission electron micrographs of articular cartilage at t0. **a**) A chondrocyte surrounded by extracellular matrix (EM); N, nucleus. **b**) High magnification detail of a chondrocyte; arrowhead, mitochondrion; asterisk, Golgi apparatus; arrows, RER; G, glycogen; N, nucleus. **c**) Chondrocyte surface surrounded by pericellular matrix (PM). **d**) Collagen fibrils (arrows) in the interterritorial matrix (IM). Scale bars: a) 500 nm; b-d) 200 nm.

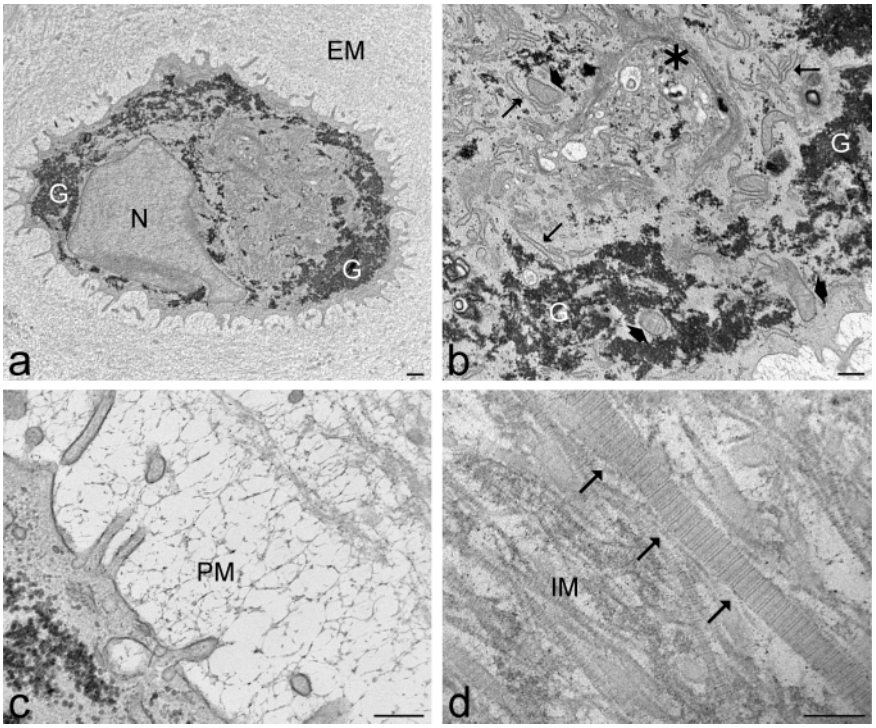

Figure 4. Transmission electron micrographs of control articular cartilage at t3. **a**) A chondrocyte surrounded by extracellular matrix (EM); note the abundant glycogen deposits (G); N, nucleus. **b**) High magnification detail of a chondrocyte; arrowheads, mitochondria; asterisk, Golgi apparatus; arrows, RER; G, glycogen. **c)** Chondrocyte surface surrounded by a loosened pericellular matrix (PM). **d**) A large collagen fibril (arrows) in the interterritorial matrix (IM). Scale bars: a) 500 nm; b-d) 200 nm.

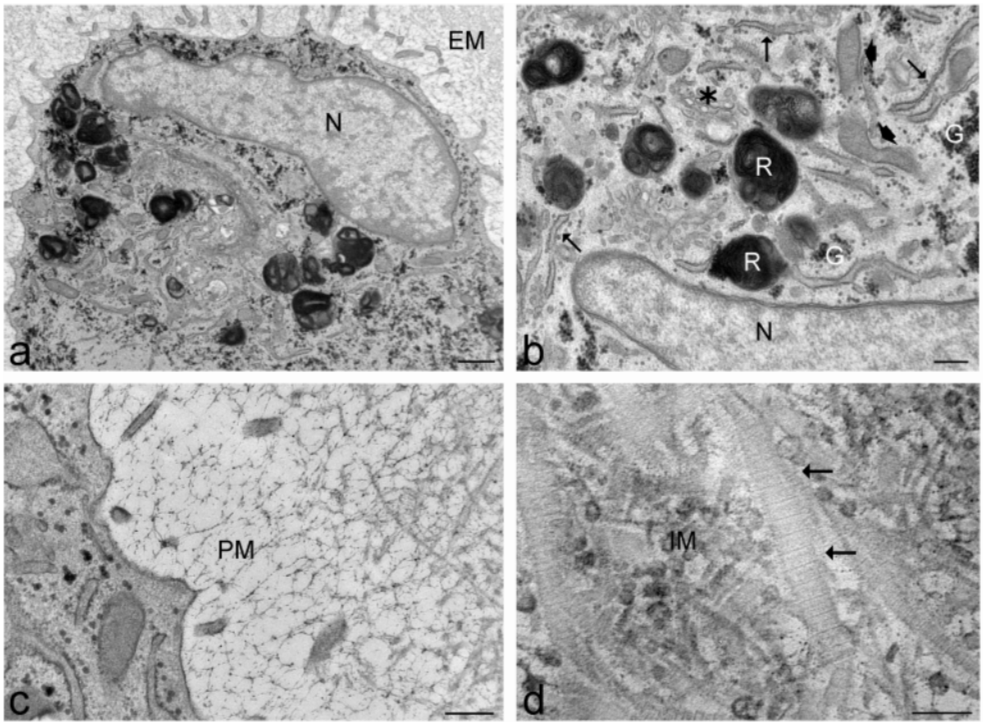

Figure 5. Transmission electron micrographs of control articular cartilage at t6. **a**) A chondrocyte surrounded by extracellular matrix (EM); N, nucleus. **b**) High magnification detail of a chondrocyte; arrowheads, mitochondria; asterisk, Golgi apparatus; arrows, RER; R, residual body. **c**) Chondrocyte surface surrounded by a loosened pericellular matrix (PM). **d**) A large collagen fibril (arrows) in the interterritorial matrix (IM). Scale bars: a) 500 nm; b-d) 200 nm.

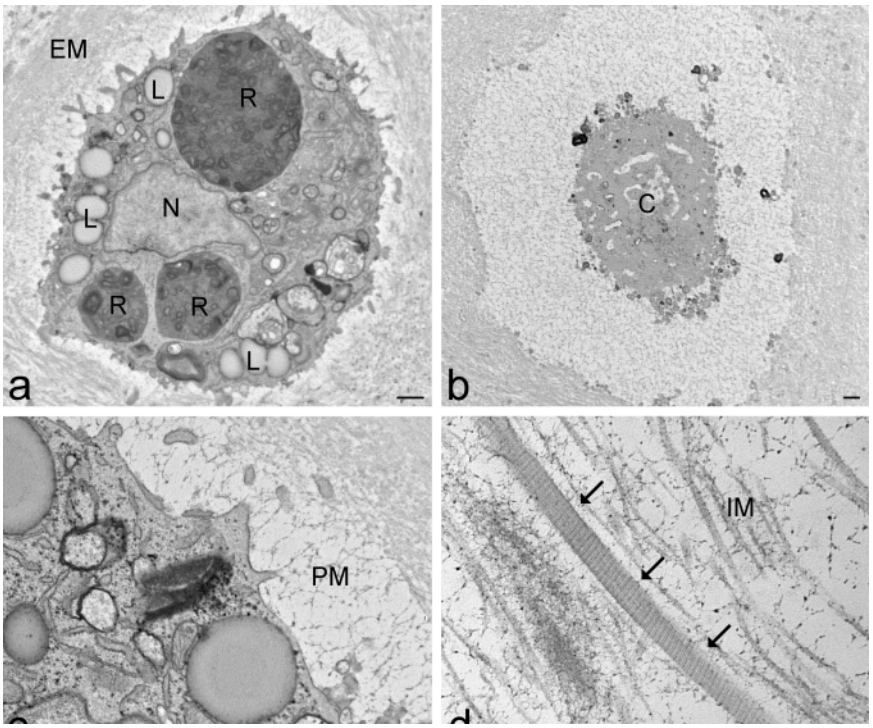

Figure 6. Transmission electron micrographs of control articular cartilage at t12. **a**) A chondrocyte surrounded by extracellular matrix (EM); note the abundant residual bodies (R) and lipid droplets (L); N, nucleus. **b**) A necrotic chondrocyte (C). **c**) Chondrocyte surface surrounded by a loosened pericellular matrix (PM). **d**) A collagen fibril (arrows) in the interterritorial matrix (IM). Scale bars: a,b) 500 nm; c,d) 200 nm.

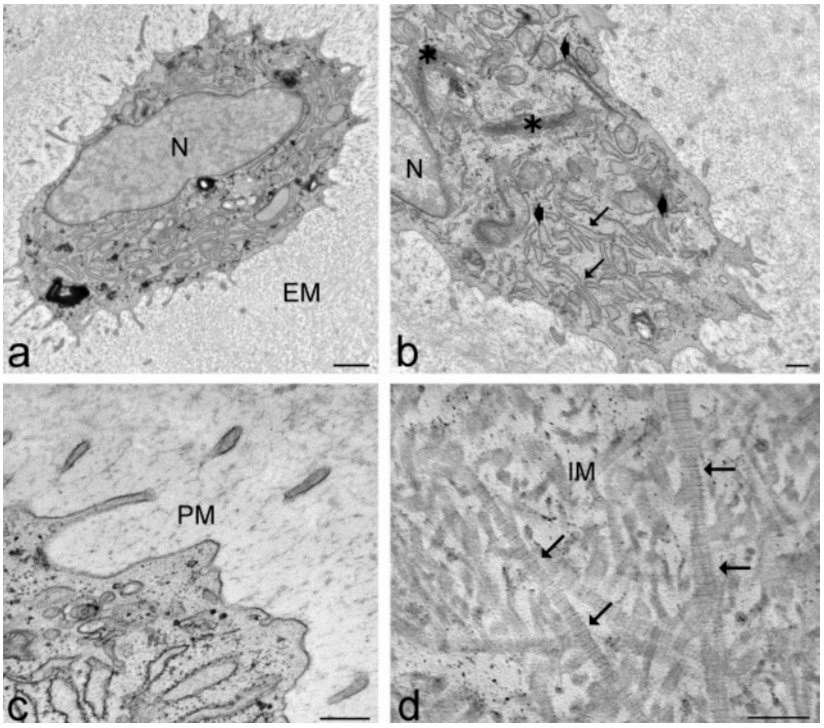

Figure 7. Transmission electron micrographs of O_3-treated articular cartilage at t3. **a**) A chondrocyte surrounded by extracellular matrix (EM); N, nucleus. **b**) High magnification detail of a chondrocyte; arrowheads, mitochondria; asterisks, Golgi apparatus; arrows, RER; N, nucleus. **c**) Chondrocyte surface surrounded by pericellular matrix (PM). **d**) Collagen fibrils (arrows) in the interterritorial matrix (IM). Scale bars: a) 500 nm; b-d) 200 nm.

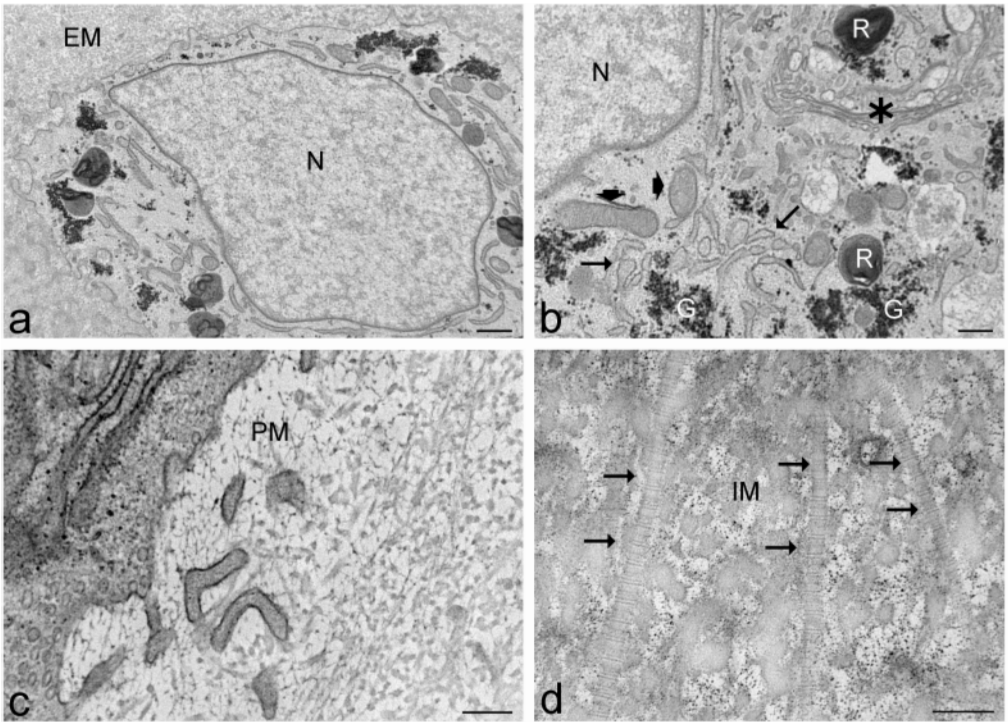

Figure 8. Transmission electron micrographs of O_3-treated articular cartilage at t6. **a**) A chondrocyte surrounded by extracellular matrix (EM); N, nucleus. **b**) High magnification detail of a chondrocyte; arrowheads, mitochondria; asterisk, Golgi apparatus; arrows, RER; G, glycogen; R, residual body; N, nucleus. **c**) Chondrocyte surface surrounded by pericellular matrix (PM). **d**) Collagen fibrils (arrows) in the interterritorial matrix (IM). Scale bars: a) 500 nm; b-d) 200 nm.

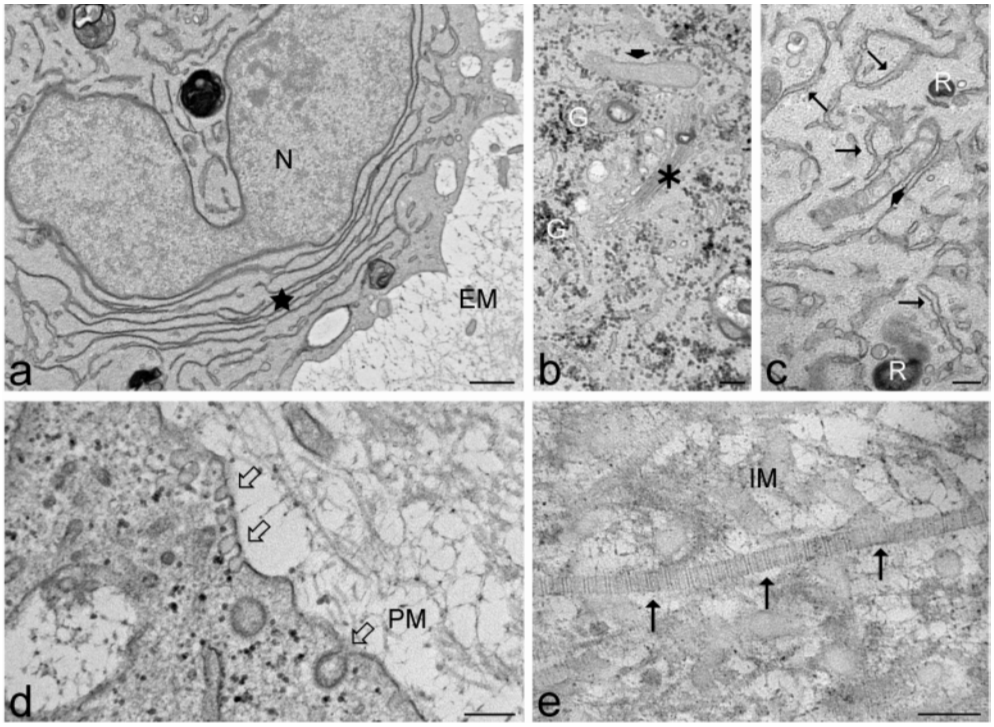

Figure 9. Transmission electron micrographs of O_3-treated articular cartilage at t12. **a**) A chondrocyte surrounded by extracellular matrix (EM); note the folded RER cisternae (star); N, nucleus. **b,c**) High magnification details of chondrocytes; arrowheads, mitochondria; asterisk, Golgi apparatus; arrows, RER; G, glycogen; R, residual body; Note the scarce presence of ribosomes on RER. **d**) Chondrocyte surface surrounded by a loosened pericellular matrix (PM); the occurrence of various vesicles (open arrows) indicates endocytic activity. **e**) A collagen fibril (arrows) in the interterritorial matrix (IM). Scale bars: a) 500 nm; b-e) 200 nm.

significantly increased (Figure 10a). The index of cell surface irregularity of control samples at t3 was similar to t0, and significantly lower at t6 and t12; the index of O_3-treated samples maintained values similar to t0 at all timepoints (Figure 10b). The granule density in the pericellular matrix of control samples was lower than t0 at all timepoints; in O_3-treated samples the density was similar to t0 at t3 and t6 but significantly decreased at t12 (Figure 10c). Collagen fibril size of control samples was significantly larger than t0 at t3 and t6, but at t12 it became similar to t0; in O_3-treated samples the fibril size values were similar to t0 at all timepoints (Figure 10d). D band length of control samples was significantly smaller than t0 at all timepoints; in O_3-treated samples the values were similar to t0 at all timepoints (Figure 10e).

Discussion

The morphological and morphometric analyses performed on healthy rabbit articular cartilage maintained *in vitro* for 12 days demonstrated a progressive alteration of both chondrocyte and extracellular matrix features in control samples, and a limited degradation in samples treated with 16 µg/mL O_3 every third day.

In control samples, chondrocytes underwent a progressive deterioration, as indicated by the accumulation of glycogen, lipid droplets, and multilamellar and residual bodies, until complete necrosis after 12 days in culture. It has been demonstrated that accumulation of glycogen may occur because of impaired ATP production.[53] In fact, since articular cartilage is a low-O_2 tissue,[54] glycolysis (*i.e.*, the anaerobic metabolism of glucose) is an important source of ATP for chondrocytes[55] and some glycogen deposits are usually present in their cytoplasm; however, if the glycolytic activity decreases (as it occurs *e.g.*, in osteoarthritis[56]) the consumption of glycogen decreases leading to its intracellular accumulation. As for lipid droplets, recent studies have associated lipid accumulation in chondrocytes to the stress-related degeneration process leading to osteoarthritis.[59,60] The progressive accumulation of multilamellar and residual bodies in the cytoplasm of control chondrocytes (from about 15% of the cytoplasm area at t3 until over 50% at t12) clearly indicates high autophagic activity.[57,58] It is likely that the environmental stress due to the *in vitro* culture would induce a progressive failure of chondrocyte metabolism accompanied by an increase in autophagic activity to limit cell damage and enable survival. Indeed, this strategy allowed cell survival until t6, but at t12 the degenerative process became too advanced and many cells underwent necrosis. The decrease in cell surface irregularity found in control samples at t6 and t12 suggests that this deterioration involves also the primary function of chondrocyte *i.e.*, the synthesis, deposition and turnover of the extracellular matrix components.[61] In fact, membrane folding together with endo/exocytic invaginations are index of molecular trafficking through the plasmalemma and their decrease may be interpreted as a lowered transmembrane transport rate.

O_3 treatment significantly improved the preservation of chondrocyte features. In fact, a significant accumulation of residual bodies in comparison to t0 was observed only at t12, although the morphometric value was significantly lower than in control untreated cells at the same timepoint. Notably, the increase of residual bodies showed the same upward trend as in control samples, but the values of O_3-treated cells were always lower, indicating a weaker stress-related autophagic activity. This suggests that O_3 is able to significantly slow down -but not to stop- the degradation process due to the preservation *in vitro*. Accordingly, no necrotic O_3-treated cells were observed at t12, although degenera-

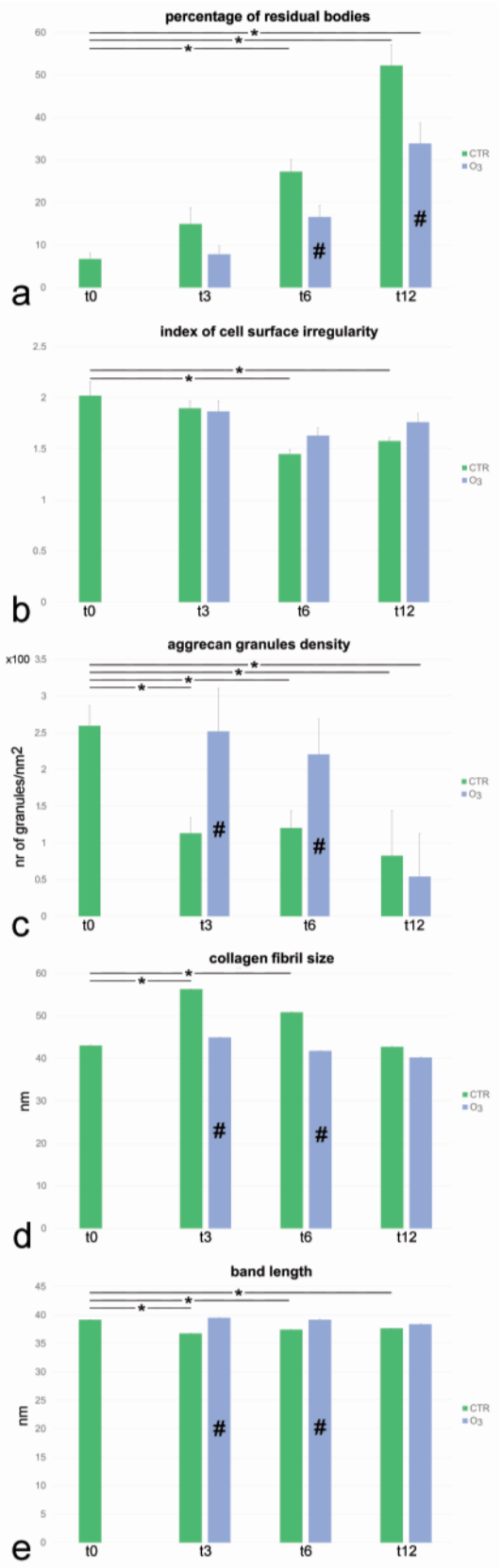

Figure 10. Results of ultrastructural morphometric analysis; mean values ± SE. Asterisk indicates statistically significant difference from t0; hashtag indicates statistically significant difference from control (CTR) at the same timepoint.

tive signs appeared at this timepoint such as RER alteration, which is suggestive of an impaired synthetic activity. O_3 prevented also the decrease of cell surface irregularity during the whole experiment, likely maintaining a high molecular transport rate.

The O_3-driven stimulation of many cytoprotective pathways through Nrf2 activation such as *e.g.*, enhancement of antioxidant enzyme activity, downregulation of pro-apoptotic factors, pro-inflammatory cytokines and autophagy, improvement of mitochondrial activity (review in [28]) presumably played a key role in ameliorating the preservation of chondrocyte structure and function under *in vitro* conditions. Moreover, it has been reported that O_3 stimulates the chondrocyte synthetic activity,[62] inducing regenerative effects in rat models of osteoarthritis.[47,48] O_3 was also found to enhance the expression of sex-determining region Y box 9 (SOX9), involved in chondrocyte differentiation, and of hypoxia-inducible factor (HIF)-1, promoting cell survival under hypoxic conditions.[63]

In the extracellular matrix, both the pericellular and interterritorial regions showed alterations in control cartilage samples. In detail, the pericellular matrix was characterized at all timepoints by a marked loosening of the molecular network, which is mostly formed of aggrecan, hyaluronan and type VI collagen[29-31] and constitutes a microenvironment responsible for the transduction of biomechanical and biochemical signals.[32,59,64] In the interterritorial matrix, a significant thickening of collagen fibrils was found from t3 to t6, but at t12 the fibril size decreased; in parallel, a significant shortening of the D band was observed at all timepoints. Distension of the pericellular matrix has been reported in aging and osteoarthritis, due to alterations (*e.g.*, cleavage, crosslinks, aggregation) of proteoglycans and collagens composing the molecular network.[31,32] Similarly, increase in size and reduction of D-band length of the collagen fibrils have been observed at the very early stage of osteoarthritis in human articular cartilage[65] and in a rabbit model of osteoarthritis.[66] It was hypothesized that collagen fibril thickening and loss of normal D-band periodicity are due to diminished intermolecular interactions finally reducing the stability of collagen fibrils.[64] Consistently, splitting of thick collagen fibrils bundles into thinner fibrils has been reported to occur only with advancing osteoarthritis.[67] All these alterations of proteoglycan and collagen molecules have been ascribed to the oxidative stress,[68,69] which is known to affect protein folding and cleavage.[70] When O_3 was applied, the loosening of pericellular matrix network was prevented until t6, while fibril size and D band length of interterritorial collagen were maintained at t0 values during the whole experiment, clearly demonstrating the effectiveness of O_3 treatment in preserving the molecular complexes responsible for the mechanical properties of the articular cartilage. The antioxidant properties of O_3 through Nrf2 activation certainly play a key role in counteracting the degradation of extracellular matrix components. Actually, it has been demonstrated that natural and synthetic compounds regulating Nrf2 are able to stimulate the expression of cartilage collagens and proteoglycans in osteoarthritis.[71] Moreover, the anti-inflammatory action of O_3 is known to downregulate in chondrocytes the stress-related secretion of interleukin 1 (IL-1), tumor necrosis factor alpha (TNF-α), IL-6, and matrix metalloproteinases,[44,60,72] which are responsible for the extracellular matrix degradation.[73] Finally, studies on *in vitro* and *in vivo* models of osteoarthritis have demonstrated that O_3 treatment increases the expression of type II collagen and aggrecan, thus limiting cartilage degeneration.[44,60,71]

The increase in proteoglycan density (as indicated by toluidine blue staining) in the interterritorial matrix of control cartilage samples at t6 and t12 could be related to the collagen size increase of about 130%: the fibrillar component of the extracellular matrix would reduce the space available to proteoglycans, thus increasing their local concentration. Moreover, as already mentioned, oxidative stress induces cartilage protein aggregation and crosslinking, while cleavage and loss of proteoglycans occur only after prolonged exposure to oxidative condition.[69] It is therefore likely that proteoglycan aggregation contributed to their retention in cartilage explants during the 12-day *in vitro* maintenance. Probably, the antioxidant properties of O_3 allowed keeping proteoglycan density at t0 levels until t6. Accordingly, it has been reported that treatment with various antioxidant agents reduces the alteration of proteoglycans and glycosaminoglycans in articular cartilage.[67,69]

Taken together, our findings demonstrate that low O_3 doses are able to influence both chondrocyte and extracellular matrix features of healthy articular cartilage explants, significantly improving their preservation *in vitro*, likely by promoting both protective and pro-regenerative pathways.

Clinical practice has demonstrated the effectiveness of O_3 administration in limiting the debilitating symptoms of degenerative joint diseases.[9,34-38] The effectiveness of O_3 in reducing pain and restoring physical function has been also compared with other therapeutic agents. Some clinical trials reported that O_3 treatment gives results similar as after corticosteroid administration,[74] but the O_3 effects were found to last longer;[75,76] however, other clinical trials reported evidence in favor of corticosteroids.[77] Some clinical trials compared the effect of intra-articular injection of O_3 and hyaluronic acid reporting similar painkilling efficacy.[78-80] When the effect of intra-articular injection of O_3 was compared with various therapeutic agents such as hyaluronic acid, platelet-rich plasma, and plasma rich in growth factor, O_3 demonstrated rapid effects but short-term results, whereas the therapeutic effect of platelet-rich plasma, plasma rich in growth factor and hyaluronic acid persisted for longer time.[40,81-84] Some studies demonstrated that O_3 and hyaluronic acid provide distinct and complementary benefits for knee osteoarthritis, O_3 offering immediate pain relief and hyaluronic acid giving sustained effects, and that their combined administration may result in a synergistic effect.[85-88] On the other hand, other studies reported that the combination of O_3 with hyaluronic acid, platelet-rich plasma or corticosteroids did not improve the treatment of temporomandibular joint osteoarthritis.[89]

It is evident that, despite some inconsistencies, the effectiveness of O_3 in reducing the painful symptoms of osteoarthritis is now firmly established by the scientific literature. However, it remains unclear whether O_3 is also able to limit cartilage deterioration or even to promote its reconstruction in patients affected by degenerative joint diseases. In this view, the results of our pilot study open promising perspectives for further investigations on the therapeutic potential of O_3 as a cartilage regenerative agent.

References

1. Schönbein CF. Ueber des Verhalten einiger organischer Materien zum Ozon. J Prakt Chem 1868;105:230-2.
2. Schönbein CF. On some secondary physiological effects produced by atmospheric electricity. Med Chir Trans 1851;34:205-20.
3. Fox CB. Ozone and antozone, their history and nature when, where, why, how is ozone observed in the atmosphere? London, J & A Churchill; 1873.
4. Kellogg JH. Diphtheria: its causes, prevention, and proper treatment. Battle Creek, Good Health Publishing Co.; 1879.
5. Bocci V, Zanardia I, Valacchi G, Borrelli E, Travagli V. Validity of oxygen-ozone therapy as integrated medication

form in chronic inflammatory diseases. Cardiovasc Hematol Disord Drug Targets 2015;15:127-38.
6. Sciorsci RL, Lillo E, Occhiogrosso L, Rizzo A. Ozone therapy in veterinary medicine: A review. Res Vet Sci 2020;130:240-6.
7. Masan J, Sramka M, Rabarova D. The possibilities of using the effects of ozone therapy in neurology. Neuro Endocrinol Lett 2021;42:13-21.
8. Oliveira Modena DA, de Castro Ferreira R, Froes PM, Rocha KC. Ozone therapy for dermatological conditions: a systematic review. J Clin Aesthet Dermatol 2022;15:65-73.
9. Jeyaraman M, Jeyaraman N, Ramasubramanian S, Balaji S, Nallakumarasamy A, Patro BP, Migliorini F. Ozone therapy in musculoskeletal medicine: a comprehensive review. Eur J Med Res 2024;29:398.
10. Hidalgo-Tallón FJ, Torres-Morera LM, Baeza-Noci J, Carrillo-Izquierdo MD, Pinto-Bonilla R. Updated review on ozone therapy in pain medicine. Front Physiol 2022;13:840623.
11. El Meligy OA, Elemam NM, Talaat IM. Ozone therapy in medicine and dentistry: a review of the literature. Dent J 2023;11:187.
12. Liu L, Zeng L, Gao L, Zeng J, Lu J. Ozone therapy for skin diseases: cellular and molecular mechanisms. Int Wound J 2023;20:2376-85.
13. Veneri F, Filippini T, Consolo U, Vinceti M, Generali L. Ozone therapy in dentistry: an overview of the biological mechanisms involved (Review). Biomed Rep 2024;21:115.
14. Ghatge SB, Asarkar A, Warghade SS, Shirsat S, Deb A. Ozone disc nucleolysis for cervical intervertebral disc herniation: a systematic review and meta-analysis. Cureus 2024;16:e59855.
15. Izadi M, Jafari-Oori M, Eftekhari Z, Jafari NJ, Maybodi MK, Heydari S, et al. Effect of ozone therapy on diabetes-related foot ulcer outcomes: a systematic review and meta-analysis. Curr Pharm Des 2024;30:2152-66.
16. Liu J, Huang Y, Huang J, Yang W, Tao R. Effects of ozone therapy as an adjuvant in the treatment of periodontitis: a systematic review and meta-analysis. BMC Oral Health 2025;25:335.
17. Machado TT, Machado ACS, Poluha RL, Proença LS, Christidis N, Parada CA, et al. The role of ozone therapy in the treatment of temporomandibular disorders: a systematic review. J Evid Based Dent Pract 2025;25:102127.
18. Ronconi G, Mariantonietta A, Codazza S, Cutaia A, Zeni A, Forastiere L, et al. Effects of oxygen-ozone injections in upper limb disorders: scoping review. J Clin Med 2025;14:2452.
19. Viebahn-Hänsler R, León Fernández OS, Fahmy Z. Ozone in medicine: the low-dose ozone concept—guidelines and treatment strategies. Ozone-Sci Eng 2012;34:408-24.
20. Sagai M, Bocci V. Mechanisms of action involved in ozone therapy: is healing induced via a mild oxidative stress? Med Gas Res 2011;1:29.
21. Niki E. Oxidative stress and antioxidants: distress or eustress? Arch Biochem Biophys 2016;595:19-24.
22. Sies H. Hydrogen peroxide as a central redox signaling molecule in physiological oxidative stress: oxidative eustress. Redox Biol 2017;11:613-9.
23. Bocci V, Aldinucci C, Mosci F, Carraro F, Valacchi G. Ozonation of human blood induces a remarkable upregulation of heme oxygenase-1 and heat stress protein-70. Mediators Inflamm 2007;2007:26785.
24. Pecorelli A, Bocci V, Acquaviva A, Belmonte G, Gardi C, Virgili F, et al. NRF2 activation is involved in ozonated human serum upregulation of HO-1 in endothelial cells. Toxicol Appl Pharmacol. 2013;267:30-40.
25. Scassellati C, Costanzo M, Cisterna B, Nodari A, Galiè M, Cattaneo A, et al. Effects of mild ozonisation on gene expression and nuclear domains organization in vitro. Toxicol In Vitro 2017;44:100-10.
26. Re L, Martínez-Sánchez G, Bordicchia M, Malcangi G, Pocognoli A, Morales-Segura MA, et al. Is ozone pre-conditioning effect linked to Nrf2/EpRE activation pathway in vivo? A preliminary result. Eur J Pharmacol 2014;742:158-62.
27. Galiè M, Costanzo M, Nodari A, Boschi F, Calderan L, Mannucci S, et al. Mild ozonisation activates antioxidant cell response by the Keap1/Nrf2 dependent pathway. Free Radic Biol Med 2018;124:114-21.
28. Malatesta M, Tabaracci G, Pellicciari C. Low-dose ozone as a eustress inducer: experimental evidence of the molecular mechanisms accounting for its therapeutic action. Int J Mol Sci 2024;25:12657.
29. Schenk RK, Eggli PS, Hunziker EB. Articular cartilage morphology. In: Kuettner KE, Schleyerbach R, Hascall V, eds. Articular cartilage biochemistry. New York, Raven Press;1986. pp. 3-22.
30. Knudson W, Aguiar DJ, Hua Q, Knudson CB. CD44-anchored hyaluronan-rich pericellular matrices: an ultrastructural and biochemical analysis. Exp Cell Res 1996;228:216-28.
31. Poole CA. Articular cartilage chondrons: form, function and failure. J Anat 1997;191:1-13.
32. Guilak F, Alexopoulos LG, Upton ML, Youn I, Choi JB, Cao L, et al. The pericellular matrix as a transducer of biomechanical and biochemical signals in articular cartilage. Ann N Y Acad Sci 2006;1068:498-512.
33. Sophia Fox AJ, Bedi A, Rodeo SA. The basic science of articular cartilage: structure, composition, and function. Sports Health 2009;1:461-8.
34. Raeissadat SA, Tabibian E, Rayegani SM, Rahimi-Dehgolan S, Babaei-Ghazani A. An investigation into the efficacy of intra-articular ozone (O_2-O_3) injection in patients with knee osteoarthritis: a systematic review and meta-analysis. J Pain Res 2018;11:2537-50.
35. Latini E, Curci ER, Nusca SM, Lacopo A, Musa F, Santoboni F, et al. Medical ozone therapy in facet joint syndrome: an overview of sonoanatomy, ultrasound-guided injection techniques and potential mechanism of action. Med Gas Res 2021;11:145-51.
36. Lino VTS, Marinho DS, Rodrigues NCP, Andrade CAF. Efficacy and safety of ozone therapy for knee osteoarthritis: an umbrella review of systematic reviews. Front Physiol 2024;15:1348028.
37. Yao TK, Lee RP, Wu WT, Chen IH, Yu TC, Yeh KT. Advances in gouty arthritis management: integration of established therapies, emerging treatments, and lifestyle interventions. Int J Mol Sci 2024;25:10853.
38. Farì G, Fai A, Donati D, Tedeschi R, Varrassi G, Ricci V, et al. The effects of oxygen-ozone therapy in knee osteoarthritis: a systematic review. J Back Musculoskelet Rehabil 2025;38:1257-66.
39. Rahimzadeh P, Imani F, Azad Ehyaei D, Faiz SHR. Efficacy of oxygen-ozone therapy and platelet-rich plasma for the treatment of knee osteoarthritis: a meta-analysis and systematic review. Anesth Pain Med 2022;12:e127121.
40. Liu Q, Liu J, Cao G, Liu Y, Huang Y, Jiang X. Ozone therapy for knee osteoarthritis: a literature visualization analysis of research hotspots and prospects. Med Gas Res 2025;15:356-65.
41. Javadi Hedayatabad J, Kachooei AR, Taher Chaharjouy N, Vaziri N, Mehrad-Majd H, Emadzadeh M, et al. The effect of ozone (O3) versus hyaluronic acid on pain and function in patients with knee osteoarthritis: a systematic review and

meta-analysis. Arch Bone Jt Surg 2020;8:343-54.
42. Zhao X, Li Y, Lin X, Wang J, Zhao X, Xie J, et al. Ozone induces autophagy in rat chondrocytes stimulated with IL-1β through the AMPK/mTOR signaling pathway. J Pain Res 2018;11:3003-17.
43. Tartari APS, Moreira FF, Pereira MCDS, Carraro E, Cidral-Filho FJ, Salgado AI, Kerppers II. Anti-inflammatory effect of ozone therapy in an experimental model of rheumatoid arthritis. Inflammation 2020;43:985-93.
44. Xu W, Zhao X, Sun P, Zhang C, Fu Z, Zhou D. The effect of medical ozone treatment on cartilage chondrocyte autophagy in a rat model of osteoarthritis. Am J Transl Res 2020;12:5967-76.
45. Sun P, Xu W, Zhao X, Zhang C, Lin X, Gong M, Fu Z. Ozone induces autophagy by activating PPARγ/mTOR in rat chondrocytes treated with IL-1β. J Orthop Surg Res 2022;17:351.
46. Yılmaz O, Bilge A, Erken HY, Kuru T. The effects of systemic ozone application and hyperbaric oxygen therapy on knee osteoarthritis: an experimental study in rats. Int Orthop 2021;45:489-96.
47. Spassim MR, Dos Santos RT, Rossato-Grando LG, Cardoso L, da Silva JS, de Souza SO, et al. Intra-articular ozone slows down the process of degeneration of articular cartilage in the knees of rats with osteoarthritis. Knee 2022;35:114-23.
48. Unlu E, Gül Satar NY, Onguncan O, Güler S, Uslu N, Ukum MO. Chondroprotective effects of ozone and hyaluronic acid in rat knee osteoarthritis: comparison of intra-articular and systemic administration. Res Vet Sci 2025;193:105798.
49. Cisterna B, Costanzo M, Nodari A, Galiè M, Zanzoni S, Bernardi P, et al. Ozone activates the Nrf2 pathway and improves preservation of explanted adipose tissue in vitro. Antioxidants (Basel) 2020;9:989.
50. Larini A, Bianchi L, Bocci V. The ozone tolerance: I) Enhancement of antioxidant enzymes is ozone dose-dependent in Jurkat cells. Free Radic Res 2003;37:1163-8.
51. Ortiz-Arrabal O, Carmona R, García-García ÓD, Chato-Astrain J, Sánchez-Porras D, Domezain A, et al. Generation and evaluation of novel biomaterials based on decellularized sturgeon cartilage for use in tissue engineering. Biomedicines 2021;9:775.
52. Darwiche SE, Tegelkamp M, Nuss K, von Rechenberg B. Histological preparation and evaluation of cartilage specimens. Methods Mol Biol 2023;2598:227-63.
53. Nishida T, Kubota S, Aoyama E, Takigawa M. Impaired glycolytic metabolism causes chondrocyte hypertrophy-like changes via promotion of phospho-Smad1/5/8 translocation into nucleus. Osteoarthritis Cartilage 2013;21:700-9.
54. Mankin HJ, Mow VC, Buckwalter JA, Iannotti JP. Form and function of articular cartilage. In: Simon SR, ed. Orthopaedic basic science. Columbus, American Academy of Orthopaedic Surgeons; 1994. pp. 1-44.
55. Lane JM, Brighton CT, Menkowitz BJ. Anaerobic and aerobic metabolism in articular cartilage. J Rheumatol 1977;4:334-42
56. Pi P, Zeng L, Zeng Z, Zong K, Han B, Bai X, Wang Y. The role of targeting glucose metabolism in chondrocytes in the pathogenesis and therapeutic mechanisms of osteoarthritis: a narrative review. Front Endocrinol 2024;15:1319827.
57. Seglen PO, Bohley P. Autophagy and other vacuolar protein degradation mechanisms. Experientia 1992;48:158-72.
58. Dunn WA Jr. Autophagy and related mechanisms of lysosome-mediated protein degradation. Trends Cell Biol 1994;4:139-43.
59. Yu J, Liu Q, Zhang Y, Xu L, Chen X, He F, et al. Stress causes lipid droplet accumulation in chondrocytes by impairing microtubules. Osteoarthritis Cartilage 2025;33:351-63.
60. Mei Z, Yilamu K, Ni W, Shen P, Pan N, Chen H, et al. Chondrocyte fatty acid oxidation drives osteoarthritis via SOX9 degradation and epigenetic regulation. Nat Commun 2025;16:4892.
61. Knudson W, Ishizuka S, Terabe K, Askew EB, Knudson CB. The pericellular hyaluronan of articular chondrocytes. Matrix Biol 2019;78-79:32-46.
62. Wu H, Wang J, Lin Y, He W, Hou J, Deng M, et al. Injectable ozone-rich nanocomposite hydrogel loaded with D-mannose for anti-inflammatory and cartilage protection in osteoarthritis treatment. Small 2024;20:e2309597.
63. Asadi S, Farzanegi P, Azarbayjani MA. Combined therapies with exercise, ozone and mesenchymal stem cells improve the expression of HIF1 and SOX9 in the cartilage tissue of rats with knee osteoarthritis. Physiol Int 2020;107:231-42.
64. Wilusz RE, Sanchez-Adams J, Guilak F. The structure and function of the pericellular matrix of articular cartilage. Matrix Biol 2014;39:25-32.
65. Shao J, Lin L, Tang B, Du C. Structure and nanomechanics of collagen fibrils in articular cartilage at different stages of osteoarthritis. RSC Adv 2014;4:51165-70
66. Maniwa S, Maeki N, Ishihara H, Takami Y, Tadenuma T, Sakai Y. Diameter of collagen fibrils in the superficial layer of osteoarthritic articular cartilage from different species. Osteoarthr Cartil 2019;27:S148-9
67. Gottardi R, Hansen U, Raiteri R, Loparic M, Düggelin M, Mathys D, et al. Supramolecular organization of collagen fibrils in healthy and osteoarthritic human knee and hip joint cartilage. PLoS One 2016;11:e0163552.
68. Tiku ML, Gupta S, Deshmukh DR. Aggrecan degradation in chondrocytes is mediated by reactive oxygen species and protected by antioxidants. Free Radic Res 1999;30:395-405.
69. Ansari MY, Ahmad N, Haqqi TM. Oxidative stress and inflammation in osteoarthritis pathogenesis: role of polyphenols. Biomed Pharmacother 2020;129:110452.
70. Hardin JA, Cobelli N, Santambrogio L. Consequences of metabolic and oxidative modifications of cartilage tissue. Nat Rev Rheumatol 2015;11:521-9.
71. Marchev AS, Dimitrova PA, Burns AJ, Kostov RV, Dinkova-Kostova AT, Georgiev MI. Oxidative stress and chronic inflammation in osteoarthritis: can NRF2 counteract these partners in crime? Ann N Y Acad Sci 2017;1401:114-35.
72. Huang P, Wang R, Pang X, Yang Y, Guan Y, Zhang D. Platelet-rich plasma combined with ozone prevents cartilage destruction and improves weight-bearing asymmetry in a surgery-induced osteoarthritis rabbit model. Ann Palliat Med 2022;11:442–51.
73. Shinmei M, Masuda K, Kikuchi T, Shimomura Y, Okada Y. Production of cytokines by chondrocytes and its role in proteoglycan degradation. J Rheumatol Suppl 1991;27:89-91.
74. Aslan SG, de Sire A, Köylü SU, Tezen Ö, Atar MÖ, Korkmaz N, et al. The efficacy of ultrasonography-guided oxygen-ozone therapy versus corticosteroids in patients with knee osteoarthritis: a multicenter randomized controlled trial. J Back Musculoskelet Rehabil 2024;37:1455-66.
75. Babaei-Ghazani A, Najarzadeh S, Mansoori K, Forogh B, Madani SP, Ebadi S, et al. The effects of ultrasound-guided corticosteroid injection compared to oxygen-ozone (O_2-O_3) injection in patients with knee osteoarthritis: a randomized controlled trial. Clin Rheumatol 2018;37:2517-27.
76. Babaei-Ghazani A, Eftekharsadat B, Soleymanzadeh H, ZoghAli M. Ultrasound-guided pes anserine bursitis injection choices: prolotherapy or oxygen-ozone or corticosteroid: a randomized multicenter clinical trial. Am J Phys Med Rehabil

2024;103:310-7.
77. Ding JB, Hu K. Injectable therapies for knee osteoarthritis. Reumatologia 2021;59:330-9.
78. Raeissadat SA, Rayegani SM, Forogh B, Hassan Abadi P, Moridnia M, Rahimi Dehgolan S. Intra-articular ozone or hyaluronic acid injection: which one is superior in patients with knee osteoarthritis? A 6-month randomized clinical trial. J Pain Res 2018;11:111-7.
79. Sconza C, Di Matteo B, Queirazza P, Dina A, Amenta R, Respizzi S, et al. Ozone therapy versus hyaluronic acid injections for pain relief in patients with knee osteoarthritis: preliminary findings on molecular and clinical outcomes from a randomized controlled trial. Int J Mol Sci 2023;24:8788.
80. Migliorini F, Giorgino R, Mazzoleni MG, Schäfer L, Bertini FA, Maffulli N. Intra-articular injections of ozone versus hyaluronic acid for knee osteoarthritis: a level I meta-analysis. Eur J Orthop Surg Traumatol 2024;35:20.
81. Duymus TM, Mutlu S, Dernek B, Komur B, Aydogmus S, Kesiktas FN. Choice of intra-articular injection in treatment of knee osteoarthritis: platelet-rich plasma, hyaluronic acid or ozone options. Knee Surg Sports Traumatol Arthrosc 2017;25:485-92.
82. de Sire A, Stagno D, Minetto MA, Cisari C, Baricich A, Invernizzi M. Long-term effects of intra-articular oxygen-ozone therapy versus hyaluronic acid in older people affected by knee osteoarthritis: A randomized single-blind extension study. J Back Musculoskelet Rehabil 2020;33:347-54.
83. Raeissadat SA, Ghazi Hosseini P, Bahrami MH, Salman Roghani R, Fathi M, Gharooee Ahangar A, Darvish M. The comparison effects of intra-articular injection of Platelet Rich Plasma (PRP), Plasma Rich in Growth Factor (PRGF), Hyaluronic Acid (HA), and ozone in knee osteoarthritis; a one year randomized clinical trial. BMC Musculoskelet Disord 2021;22:134.
84. Sconza C, Parente A, Marotta N, Farì G, Scaturro D, Vecchio M, et al. Intra-articular injections of oxygen-ozone versus hyaluronic acid for the treatment of knee osteoarthritis: a randomized controlled trial. J Back Musculoskelet Rehabil 2025:10538127251358732.
85. Giombini A, Menotti F, Di Cesare A, Giovannangeli F, Rizzo M, Moffa S, Martinelli F. Comparison between intrarticular injection of hyaluronic acid, oxygen ozone, and the combination of both in the treatment of knee osteoarthrosis. J Biol Regul Homeost Agents 2016;30:621-5.
86. Silva Júnior JIS, Rahal SC, Santos IFC, Martins DJC, Michelon F, Mamprim MJ, et al. Use of reticulated hyaluronic acid alone or associated with ozone gas in the treatment of osteoarthritis due to hip dysplasia in dogs. Front Vet Sci 2020;7:265.
87. Akhavanakbari G, Asayeshi M, Noktehsanj R, Aslani MR. Comparing the efficacy of combining ozone therapy with hyaluronic acid versus using hyaluronic acid alone for pain relief in patients with knee osteoarthritis: A randomized clinical trial. Complement Ther Med 2025;93:103238.
88. Latini E, Nusca SM, Curci ER, Lacopo A, Di Stasi V, Santoboni F, et al. Ozone and hyaluronic acid, alone and in combination: exploring temporal dynamics and synergies in intraarticular therapy for knee osteoarthritis. Pain Physician 2025;28:347-57.
89. Cömert Kiliç S, Babayev U, Kiliç N. Is intra-articular injection of hyaluronic acid, corticosteroid or platelet-rich plasma following medical ozone superior to medical ozone alone in the treatment of temporomandibular joint osteoarthritis? J Oral Maxillofac Surg 2025;83:1068-77.

Received: 12 November 2025. Accepted: 30 November 2025.

European Journal of Histochemistry 2026; 70:4440
doi:10.4081/ejh.2026.4440